Electronic Supplementary Material (ESI) for Molecular BioSystems.
This journal is © The Royal Society of Chemistry 2015

Supplementary information

Figure S1. Expression of BAMBI and BTG2 upon estrogen and retinoic acid treatments. RT-qPCRs directed against BAMBI and BTG2 performed on total RNAs extracted from MCF-7 cells treated for 3 hours with vehicle (v), 10nM estradiol (E2), 100nM RAR agonists AM580/CD437 (RA) or a mixture of E2 (10nM) and AM580/CD437 (100nM) (RA+E2).

Figure S2. Probing the functional consequences of the E2/RA antagonism on miRNA genes (A) Functional annotation of the validated targets of the miR-23a/24-2, miR-210 (orange) and miR-17/92, miR-424/450b (blue) with the GeneGo Pathway maps algorithm. (B) Functional annotation of the validated targets of the miR-23a/24-2, miR-210 (orange) and miR-17/92, miR-424/450b (blue) with the GeneGo Metabolic Networks algorithm. (C) Functional annotation of the genes down-regulated by RA and up-regulated by E2 according to [1] with the GeneGo Pathway maps algorithm. (D) Functional annotation of the genes down-regulated by RA and up-regulated by E2 according to [1] with the GeneGo Metabolic Networks.

Figure S3. RA perturbs mitochondrial activity and respiration in MCF-7 cells. Response of oxygen consumption rate (OCR) measured in real-time after injection of oligomycin, FCCP, rotenone and antimycin using a Seahorse Bioscience XF24 extracellular flux analyzer (see materials and methods for details). Data shown are the average of 3 independent experiments. Indicated results were first normalized to protein concentration then to the baseline at the time point prior to compound injections.

Figure S4. Effect of estrogen and retinoic acid on MDA-MB-231 cells and primary HMEC. (A) Extracellular lactate production measured in the supernatant of MDA-MB-231 cells and HMEC after 48 hours of the indicated treatments. (B) RT-qPCRs directed against the indicated miRNAs performed on total RNAs extracted from MDA-MB-231 cells and HMEC treated for 3 hours with 10nM E2, 100nM AM580/CD437 or a mixture of E2 (10nM) and AM580/CD437 (100nM). (C) Cell morphology of MCF-7 and MDA-MB-231 cells after 3 days treatment with RA agonists (top). Measure of Annexin V (bottom). (D) Western blot directed against ESR1 in HMEC, MDA-MB-231 and MCF-7 cells. The tubulin was also revealed to assess control loading.

Figure S5. Gene expression levels in breast tumors. The mean expression level of the indicated genes was calculated over the main molecular subgroups characterized in [2] (CIT) and [3] (NKI). For each gene, non-parametric Kruskal-Wallis tests indicated that $p<0.0001$. Information about the expression of RXRB and RXRG are not available in the NKI dataset [3].

Figure S6. c-Myc-centered network regulating cell metabolism. c-Myc is able to repress the miR-23a/24-2 transcription [4] while the miR-24 inhibits c-Myc expression [5] (feed-back loop, FBL). Concomitantly, c-Myc induces the expression of LDHA at both the transcriptional [6, 7] and post-transcriptional levels (feed-forward loop, FFL).

Supplementary Table S1. List of primers used in this study

Supplementary Table S2. List of all potential ESR1 binding sites (independently of the score used in MIR@NT@N) located in the sequences upstream the miR-23a/24-2, miR-210, miR-17/92 and miR-424/450b.

Supplementary Table S3. Description of the reverse engineering approach used to predict E2/RA regulation of miRNA genes from expression profiles of predicted targets.

Supplementary Table S4. Validated targets of the miR-23a/24-2, miR-210, miR-17/92 and miR-424/450b extracted from the miRTarBase database.

Supplementary Table S5. Functional annotation of the genes down-regulated by RA and up-regulated by E2 using the DAVID resource.

References

1. S. Hua, R. Kittler and K. P. White, *Cell*, 2009, 137, 1259-1271.
2. M. Guedj, L. Marisa, A. de Reynies, B. Orsetti, R. Schiappa, F. Bibeau, G. Macgrogan, F. Lerebours, P. Finetti, M. Longy, P. Bertheau, F. Bertrand, F. Bonnet, A. L. Martin, J. P. Feugeas, I. Bieche, J. Lehmann-Che, R. Lidereau, D. Birnbaum, F. Bertucci, H. de The and C. Theillet, *Oncogene*, 2011.
3. C. Fan, D. S. Oh, L. Wessels, B. Weigelt, D. S. Nuyten, A. B. Nobel, L. J. van't Veer and C. M. Perou, *N Engl J Med*, 2006, 355, 560-569.
4. P. Gao, I. Tchernyshyov, T. C. Chang, Y. S. Lee, K. Kita, T. Ochi, K. I. Zeller, A. M. De Marzo, J. E. Van Eyk, J. T. Mendell and C. V. Dang, *Nature*, 2009, 458, 762-765.
5. A. Lal, F. Navarro, C. A. Maher, L. E. Maliszewski, N. Yan, E. O'Day, D. Chowdhury, D. M. Dykxhoorn, P. Tsai, O. Hofmann, K. G. Becker, M. Gorospe, W. Hide and J. Lieberman, *Mol Cell*, 2009, 35, 610-625.
6. H. Shim, C. Dolde, B. C. Lewis, C. S. Wu, G. Dang, R. A. Jungmann, R. Dalla-Favera and C. V. Dang, *Proc Natl Acad Sci U S A*, 1997, 94, 6658-6663.
7. B. C. Lewis, H. Shim, Q. Li, C. S. Wu, L. A. Lee, A. Maity and C. V. Dang, *Mol Cell Biol*, 1997, 17, 4967-4978.

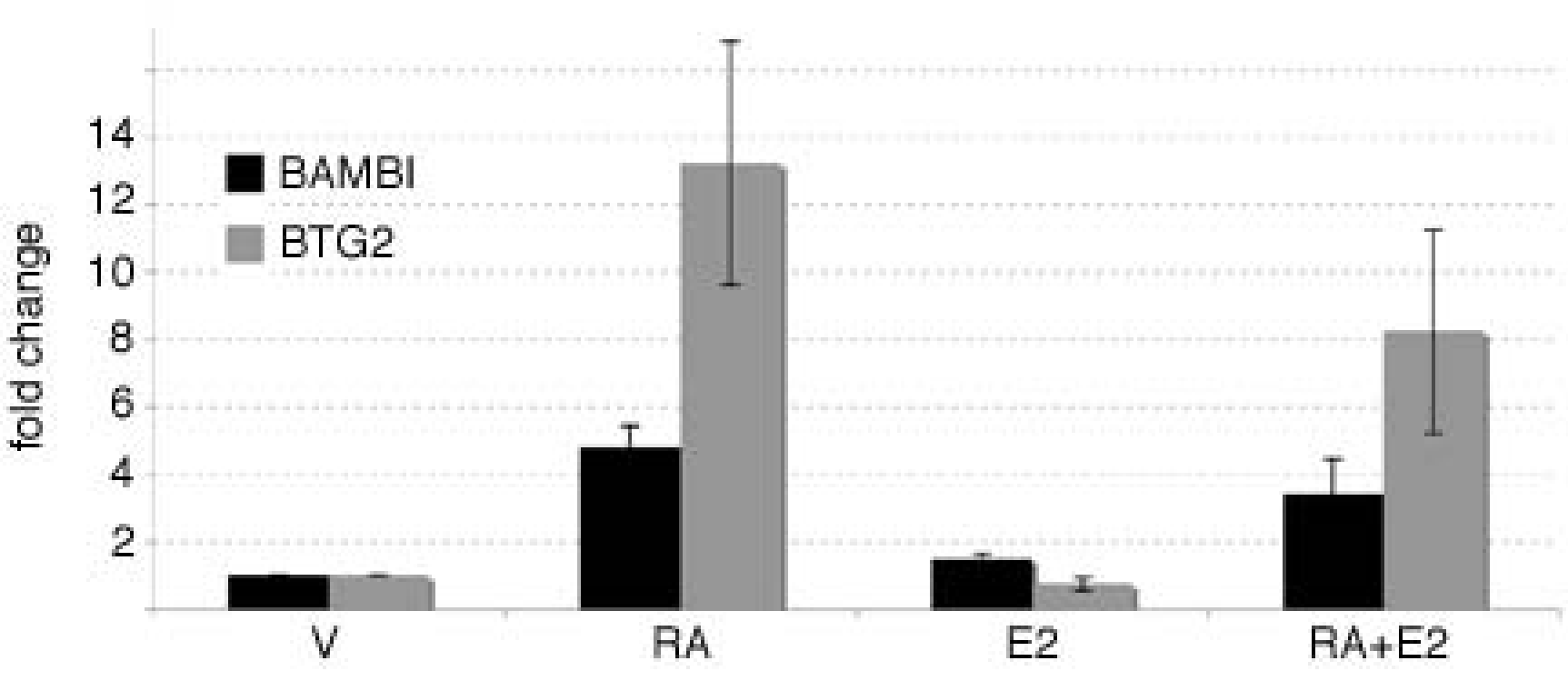

Saumet et al., Figure S1

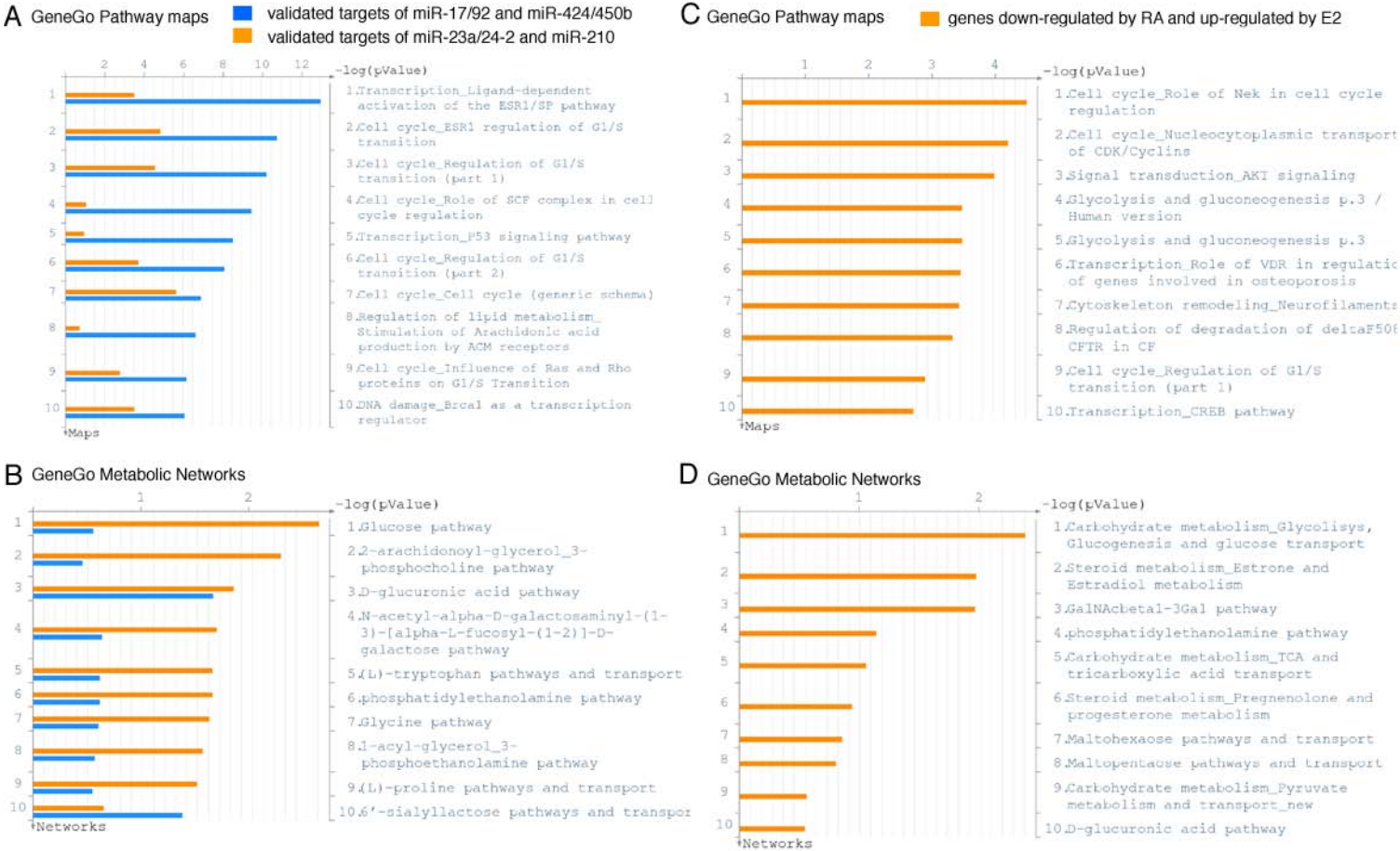

Saumet et al., Figure S2

	Basal Respiration		(pMoles/min)	Proton Leak		(pMoles/min)	ATP Production		(pMoles/min)	Maximal Respiration		(pMoles/min)
	MEAN	±	SEM	MEAN	±	SEM	MEAN	±	SEM	MEAN	±	SEM
vehicle	34	±	1	20	±	2	14	±	1	46	±	4
RA	27	±	1	17	±	1	9	±	0	27	±	2
E2	34	±	3	21	±	1	13	±	2	44	±	4
RA + E2	24	±	1	15	±	0	9	±	1	23	±	1

Saumet et al., Figure S3

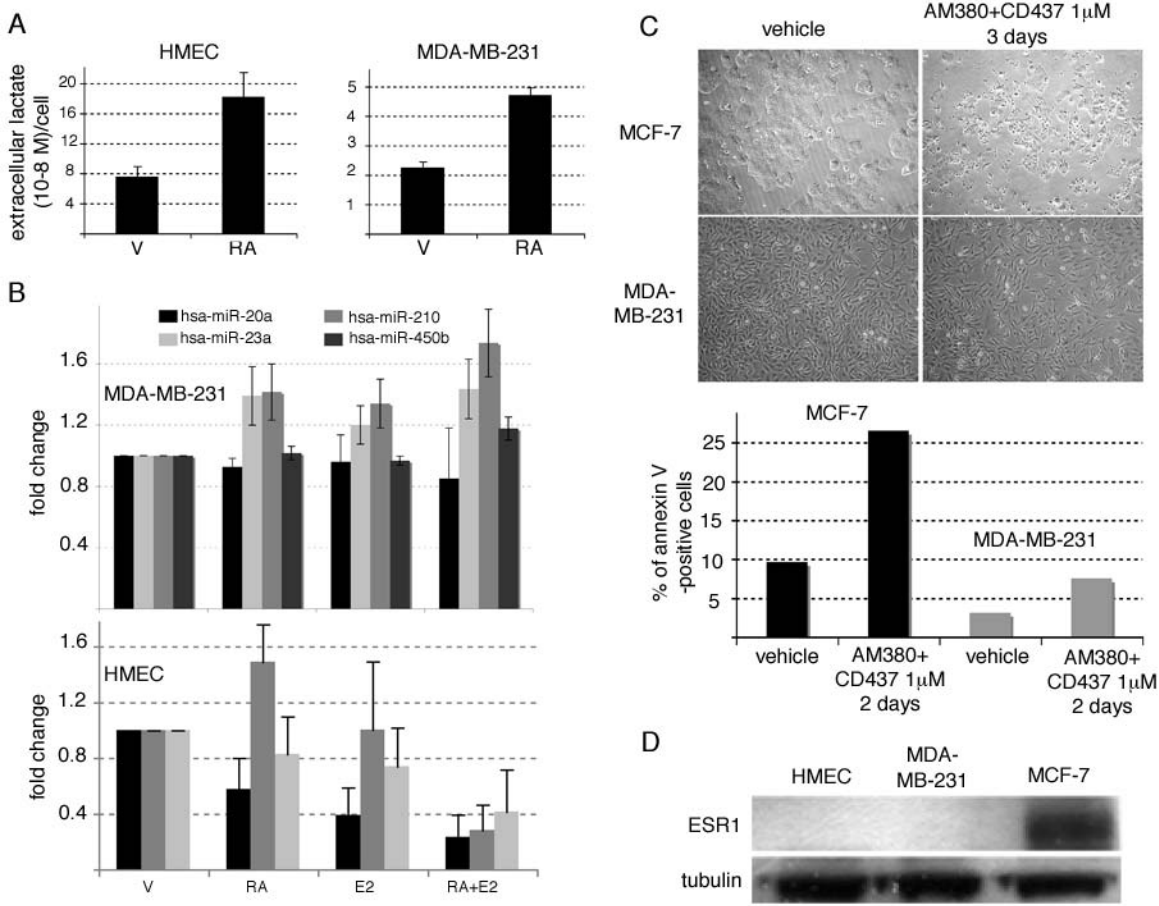

Saumet et al., Figure S4

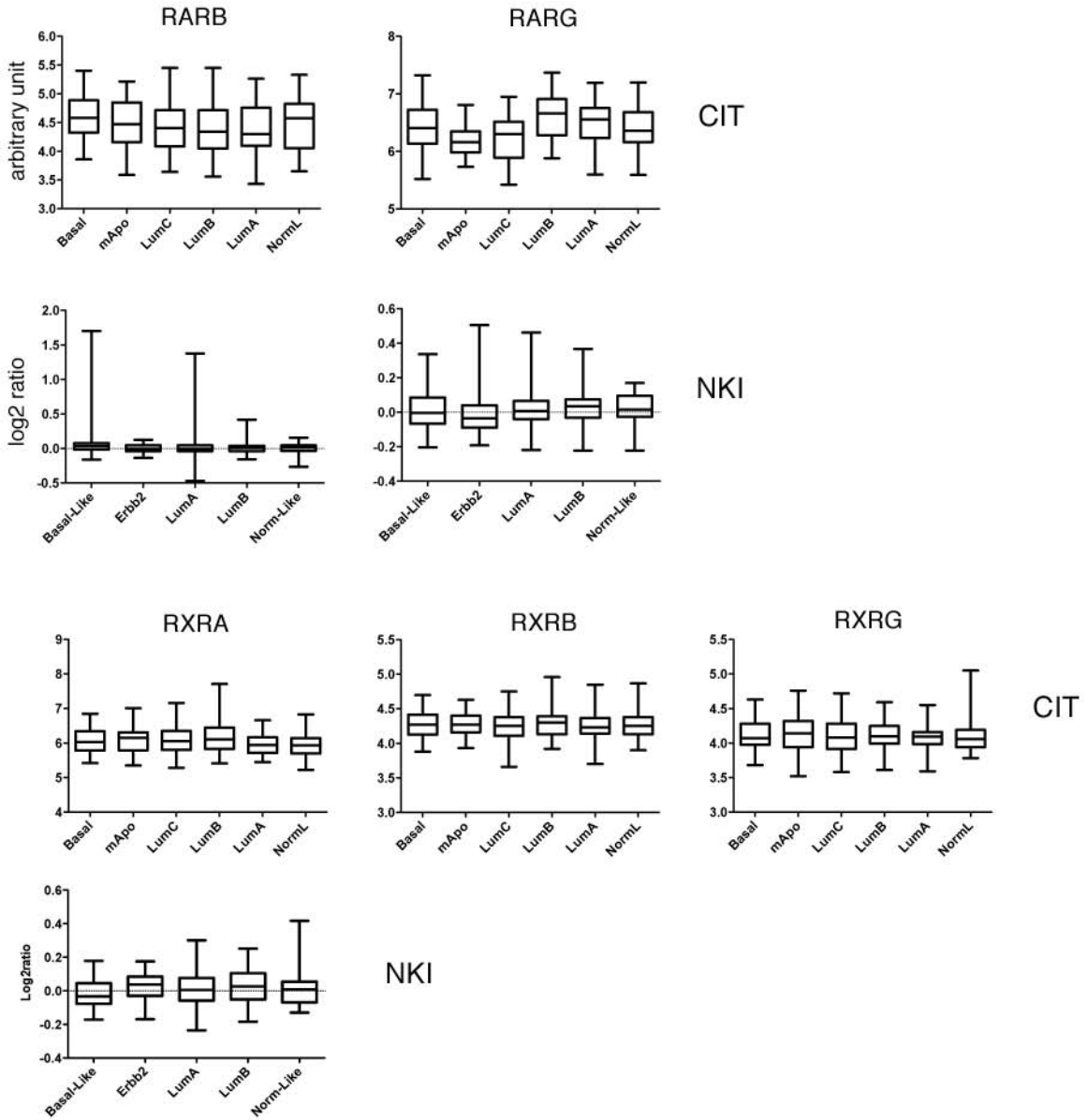

Saumet et al. Figure S5

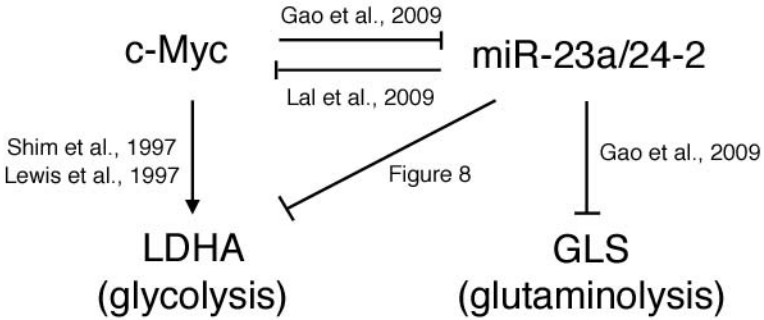

Feed-Back Loop

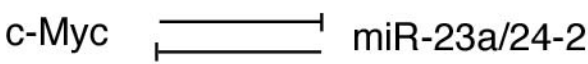

Feed-Forward Loop

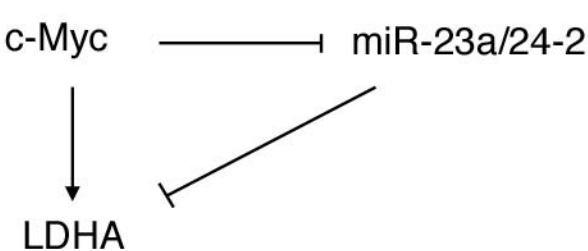

Saumet et al., Figure S6